

MAGNETIC RESONANCE IMAGING FINDINGS OF GRANULOSA CELL TUMOR OF THE OVARY

Shigenobu Motoshima,¹ Hiroyuki Irie,² Takahiko Nakazono,² Fumio Yamasaki,³ Yoshifumi Nakao,⁴ Masatoshi Yokoyama,⁴ Naofumi Okura¹

¹ Department of Obstetrics and Gynecology, Kokura Medical Centre, Japan

² Department of Radiology, Faculty of Medicine, Saga University, Japan

³ Department of Pathology, Takagi Hospital, Japan

⁴ Department of Obstetrics and Gynecology, Faculty of Medicine, Saga University, Japan

PJR April - June 2012; 22(2):46-51

Introduction

Ovarian granulosa cell tumor (GCT) is a low-grade malignant tumor, and the most common functioning ovarian tumor.^{1,2} For most patients, surgery alone is sufficient primary therapy.² However, GCT is potentially aggressive. Between 10-50% of patients develop recurrences,¹ and when GCT does recur, it can progress quite rapidly.² The most important prognostic factor is tumor stage^{1,3} and tumor size has also been known to influence prognosis.⁴ In addition, when functional most GCT are estrogenic (70%), but rarely, androgenic effects may be present as well.^{1,3-6} When the tumor is functional, a typical endometrial effect is cystic hyperplasia usually exhibiting some degree of precancerous atypia, and carcinoma occurs in less than 5% of cases.²⁻⁵ Evaluation of the uterine endometrium is also important.⁷

Thus, preoperative diagnosis of GCT is clinically important.^{1,8} Although it is relatively rare, GCT accounts for approximately 1.5% of all ovarian tumors,¹ and its rarity makes it difficult to clarify clinical course and provide adequate treatment, leading to large tumors at diagnosis.^{3,5,8} There are only a few reports of the magnetic resonance imaging (MRI) characteristics of GCT^{6,9} and to the best of our knowledge, there is no well-organized report about dynamic contrast enhanced (DCE) and diffusion weighted image (DWI) in the MRI

evaluation of GCT.

The purpose of the present study was to evaluate the MRI findings of GCT and compare them to previously documented reports. In addition to the conventional morphological imaging assessment, we also evaluated functional imaging, including DCE-and DWI-MRI.

Materials and Methods

Cases

From January 2005 to December 2009, consecutive six ovarian tumors were diagnosed pathologically as GCT at Saga University Hospital. Clinical courses, MRI findings, and pathological findings for each patient were retrospectively reviewed. All patients underwent MRI examination at Saga University Hospital.

Clinical Course

For each patient, age at diagnosis, menstrual status, presentation, serum sex hormone levels before and after operation- estrogen (estradiol (E2)) (n=5) and androgen (testosterone (T4)) (n=3), and operative methods were reviewed from their medical charts.

MRI Technique

The MRI examinations were performed using a 1.5 Tesla or 3 Tesla MRI units. In all cases, imaging sequences were T1-weighted image (T1WI), T2-weighted image (T2WI), and fat-suppressed T1-weighted

Correspondence : Dr. Shigenobu Motoshima
Department of Obstetrics and Gynecology,
Kokura Medical Centre
10-1, Harugaoka, Kokura minami-ward,
Kitakyushu-city, Fukuoka 8028533, Japan
Tel: +81-93-921-8881 Fax: +81-93-922-5072
E-mail: s.motoshima@gmail.com

image (FS-T1WI). Five of six patients underwent DCE imaging following the intravenous administration of gadopentetate dimeglumine (Magnevist; Schering, Germany) at a dose of 0.1 mmol/kg body weight. Images were obtained at 0, 30, 60, 120, and 180 seconds post-injection. After February 2007, two of the six patients underwent DWI (b= 1000s/mm²) and apparent diffusion coefficient (ADC) map.

Imaging Analysis

The following findings were determined via MRI: (1) tumor size—maximum diameter of the tumor; (2) morphologic pattern- the solid-dominant type containing a solid part of more than 50%, the cyst-dominant type containing solid part less than 50%, and the totally cystic type containing a solid part; (3) hemorrhage-high signal intensity on FS-T1WI in the cystic contents; (4) signal intensity on T1WI and (5) T2WI of solid part compared to the muscle; (6) pattern of DCE: early enhancement or prolonged enhancement; (7) signal intensity on DWI of solid part compared to the serous fluid (urine or cerebrospinal fluid (CSF)); (8) ADC value (x10⁻³ mm²/s) of solid part on ADC map; (9) uterine endometrial thickness (mm) measured on sagittal T2WI.

Pathological Analysis

The dominant histologic pattern and the cellularity of solid part in each case were analyzed. Uterine endometrium from hysterectomy specimens were analyzed pathologically, and all pathological findings were analyzed by a single pathologist.

Results

All tumors were unilateral and adult type. Age of patients ranged from 37 to 82 years (median 64 years). Five of six patients were postmenopausal. Presentation of patients were atypical uterine bleeding (n=4), secondary amenorrhea (n=1), and incidental (n=1). Preoperative serum estradiol (E2) levels (n=5) and testosterone (T4) levels (n=3) were measured. None of the patients took exogenous estrogen agent. The serum estradiol level (normal range not more than 10pg/ml) ranged from 16.1 to 144pg/ml (median 49pg/ml) in four postmenopausal patients and 26pg/ml in one premenopausal patient. Three of four post-

menopausal patients showed higher serum estrogen levels and decreased-to-normal range after surgery. The serum testosterone level (normal range from 0.06 to 0.86ng/ml) ranged from 0.23 to 1.16ng/ml (median 0.34ng/ml). One of the three patients showed higher serum testosterone level and decreased to normal range after surgery. All postmenopausal patients (n=5) underwent transabdominal hysterectomy and bilateral salpingo-oophorectomy. One premenopausal patient underwent unilateral salpingo-oophorectomy. The clinical courses for each case are summarized in (Tab.1).

Case	Age at diagnosis (years old)	Menstrual status	Presentation *	Hormone level **	Operative method ***
1	82	38 years post-menopause	AGB	E2: 144 T4: 0.23	TAH+BSO
2	73	31 years post-menopause	AGB	E2: 80 T4: 0.34	TAH+BSO
3	60	5 years post-menopause	Incidental	E2: N/A T4: N/A	TAH+BSO
4	37	Premenopausal	Secondary amenorrhea	E2: 26 T4:1.16	USO
5	68	13 years post-menopause	AGB	E2: 49 T4: N/A	TAH+BSO
6	52	2 years post-menopause	AGB	E2:16.1 T4: N/A	TAH+BSO

Table 1: *AGB: atypical genital bleeding, ** E2: estradiol (not more than 10pg/ml), T4: testosterone (0.06~0.86ng/ml), N/A: not available, ***TAH: transabdominal hysterectomy, BSO: bilateral salpingo-oophorectomy, USO: unilateral salpingo-oophorectomy

Maximum tumor diameter ranged from 3.9 to 20.1cm (median 7.3cm), and morphological patterns varied. Five cases were admixture of cystic and solid components, predominantly solid (Case 1: Fig.1, Case 2: Fig.2) in three, predominantly cystic in two, and totally

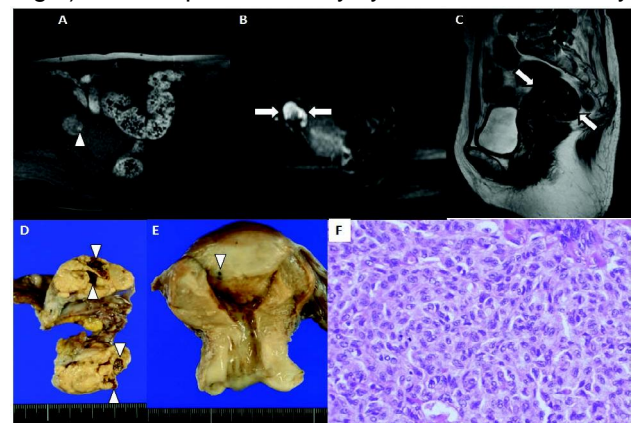


Figure 1

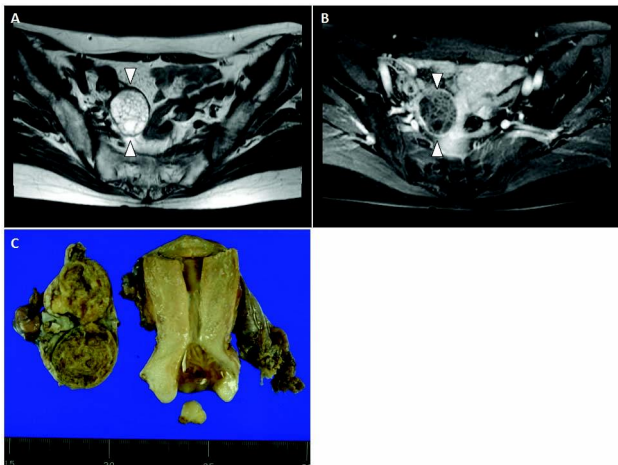


Figure 2

cystic (Case 3: Fig.3) in one. Four of six cases showed high signal intensity on FS-T1WI, representing hemorrhage in the tumor. Signal intensity of solid part on T2WI showed heterogeneously slightly-high to high

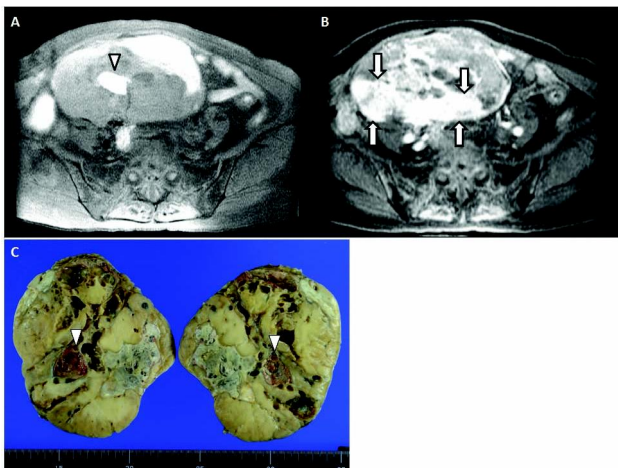


Figure 3

in all cases. On DCE, four of five cases showed early enhancement and the remaining one showed prolonged enhancement. Two of six tumors underwent DWI, and both showed high signal intensity on DWI and low ADC value on ADC map. Endometrial thickness ranged from 2.6 to 13.5mm (median 3.7mm). Abnormal endometrial thickness was defined as greater than 6mm in the present study, as most studies agree that an endometrial thickness of 5mm or less in a postmenopausal woman is consistent with atrophy.¹⁰ Only one case showed abnormal endometrial thickness among five menopausal cases. The MRI findings for each case are summarized in (Tab. 2).

Case	Tumor diameter (mm)	Morphologic pattern	Hemorrhage	T1WI * (S.I.) *****	T2WI ** (S.I.) *****	DWI *** (S.I.) *****	ADC value **** (x10 ⁻³ mm ² /s)	Enhancement pattern	Uterine endometrial thickness (mm)
1	120	Solid-dominant	+	Low	Slightly high to high	N/A	N/A	Early enhancement	4.0
2	33	Cyst-dominant	+	Low	Slightly high to high	High	0.96	Early enhancement	2.6
3	39	Entirely cystic	-	Low	Slightly high to high	N/A	N/A	Early enhancement	2.6
4	51	Solid-dominant	-	Low	Slightly high to high	High	0.96	Early enhancement	4.2
5	201	Solid-dominant	+	Low	Slightly high to high	N/A	N/A	Early enhancement	3.3
6	97	Cyst-dominant	+	Low	Slightly high to high	N/A	N/A	Early enhancement	13.5

Table 2: *T1WI; T1-weighted image, **T2WI; T2-weighted image, ***DWI; diffusion weighted image, ****ADC; apparent diffusion coefficient, *****S.I.; signal intensity, *****N/A; not available

The dominant histologic pattern was insular pattern (n=2), diffuse pattern (n=2), macrofollicular (n=1), and microfollicular (n=1). Cellularity of the solid part in the tumor was high (n=5). Pathological analysis of the uterine endometrium from the hysterectomy specimens was undertaken in five patients. One patient showed simple hyperplasia and the remaining four patients showed no atypical lesion. The pathological findings for each case are summarized in (Tab. 3).

Case	Dominant pathologic pattern	Cellularity of solid part	Uterine endometrium
1	Insular	Hyper	No atypical lesion
2	Diffuse	Hyper	No atypical lesion
3	Macrofollicular	N/A	No atypical lesion
4	Diffuse	Hyper	N/A
5	Microfollicular	Hyper	No atypical lesion
6	Insular	Hyper	Simple hyperplasia

Table 3: N/A; not available

Discussion

GCT is classified as a sex cord-stromal tumor in the World Health Organization (WHO) histological classification of ovarian tumors.¹ Sex cord-stromal tumors

may manifest as solid, mixed solid and cystic, or cystic masses in rare cases, whereas malignant epithelial tumors are primarily cystic and may be associated with varying protrusions of solid component.¹¹ GCT is commonly encapsulated, with a smooth or lobulated surface,^{1,2} and morphological findings have been described as a variable admixture of cystic and solid parts,^{4,8} from predominantly cystic^{3,5} to predominantly solid with variable amounts of cystic components.¹ These variable morphologic findings may be due to the variety of histologic patterns (microfollicular, macrofollicular, insular, trabecular, cylindromatous, watered silk, and diffuse).^{1,4,5,12} Most solid part showed heterogeneous appearances due to the associated hemorrhage, necrosis, or fibrosis of the tumor.¹³ Morphologically, a small percentage (3%) is totally cystic—either uniloculated or multiloculated—resembling cystadenoma.^{1,4,5} Moreover, hemorrhage is common and characteristic of GCT, resulting in fibrosis with deposition of blood pigment.^{4,5} MRI is very sensitive to detecting hemorrhage, and the signal intensity reflects the age of the hematoma.¹⁴ To reflect these macroscopic findings, MRI findings of GCT showed that admixed solid and multiple cystic adnexal mass as well as cyst of filled with hemorrhage associated with uterine changes.^{6,9} These MRI findings are characteristic of GCT, although not specific.^{6,9} In the present study, morphologic MRI appearances consisted of admixture of heterogeneous solid and multilocular cystic contents with hemorrhage in most cases, including one tumor that was totally cystic with multilocular. MRI findings of the cases coincide in general with the characteristic MRI findings as reported in the previous literatures.

DCE and DWI can be used to assess the vascular characteristics and molecular diffusion of tumors, respectively.¹⁵ In addition to conventional morphological imaging, we also analyzed the cases on functional MRI, including DCE and DWI. In the present study, four of five cases showed early enhancement (Case1: Fig.1). Evaluation of the Doppler flow patterns of GCT on ultrasonography showed a low resistive index in the previous report.¹³ This finding suggests that the GCT has high vascularity which would reflect the findings of early enhancement on DCE in the present study. Other sex-cord stromal tumors of DCE reported include fibroma and sclerosing stromal tumor.^{16,17} Fibroma shows weak and late enhancement,¹⁶ and sclerosing stromal tumor shows early peripheral

enhancement with centripetal progression.¹⁷ Restricted diffusion, which shows high signal intensity on DWI coincident with a low ADC value, may represent hypercellularity of solid part. DWI is expected to be able to differentiate between benign or malignant ovarian solid tumors¹¹ as malignant lesions have high cellularity in general. According to Takeuchi et al,¹¹ ovarian malignant solid component showed high signal intensity on DWI and significantly lower ADC value compared to benign solid part. In the present study, both cases of solid part showed restricted diffusion and pathologically-confirmed high cellularity (Case 2: Fig.2). This pathological high cellularity may reflect a restricted diffusion. And the remaining three cases which have solid part also showed pathological high cellularity. Results obtained by DWI were also consistent with the hypothesis that restricted diffusion may be the cause of this characteristic MRI finding, although cases tested were limited to two. Early enhancement on DCE and restricted diffusion on DWI may be one of the MRI indicators of GCT.

Most patients with GCT have sex hormone-related symptoms.⁸ GCT is the most common estrogenic ovarian tumor.^{4,5} The symptoms and clinical manifestation related to estrogenic change vary depending on the patient's age and reproductive status. For postmenopausal women, atypical genital bleeding is frequently present and for women of reproductive age, most patients have menstrual irregularities or secondary amenorrhea.^{1-3,5} Enlargement of the uterus and endometrial thickening might be seen as a result of the estrogen production of the tumor.¹ Other estrogenic effects can include tenderness or swelling of the breast, and vaginal cytology may show an increase in maturation of squamous cells.³ Besides serum estradiol, Inhibin B and anti-Müllerian hormone (AMH) have been suggested as tumor markers of GCT, although they are not specific.^{6,8,18} Androgenic effects such as virilization or hirsutism may also be present.^{3,5} There is also a nearly 50% frequency of a cystic morphological appearance of tumors associated with androgenic manifestations.^{4,5} The nature of the association between androgen production and the formation of thin-walled cyst is an enigma.⁴ In the present study, among five postmenopausal cases, serum estrogen levels were examined in four and were high in all tested cases. Among four estrogen-producing tumor cases, only one showed abnormal endometrial thickness. In one of the three cases who did not show an abnormal endometrial thickness, pathological


findings of resected uterus confirmed adenomyosis and suggested an estrogen activation of uterine endometrium despite being 31 years post-menopause (Case 2: Fig.2). Also, one case with elevated serum androgen level showed no evidence of polycystic ovary through imaging and showed no clinical androgenic effect. The other estrogen-producing tumors are thecoma, and sclerosing stromal tumor, and the other androgen-producing tumors are Sertoli-Leydig cell tumor, thecoma, sclerosing stromal tumor, gynandroblastoma, and metastatic ovarian tumor.^{19,20} In the present study, we were unable to demonstrate an association between estrogen-producing cases and abnormal endometrial thickness in most cases. One possible reason for an estrogen-producing tumor case that did not display abnormal endometrial thickness may be due to the ten years elapsed since menopause.

Conclusion

GCT is a relatively rare low-grade malignant tumor, but preoperative diagnosis is possible if characteristic findings can be detected via MRI. Additionally, DCE and DWI-MRI can assist diagnosis of GCT. Recognition of indicators from MRI findings of adnexal mass, as well as comprehensive evaluation and inclusion of serum tumor marker and serum sex hormone levels may confirm diagnosis of GCT and can contribute to a better prognosis through determination of a precise management strategy.

References

1. Tavassoli FA, Mooney E, Gersell DJ, McCluggage WG, Konishi I, Fujii S, et al. Sex cord-stromal tumours. In: Tavassoli FA, Devilee P, editors. Pathology and genetics tumours of the breast and female genital organs. World Health Organization classification of tumours. Lyon: IARC Press; 2003. p. 146-61.
2. Berek JS, Longacre TA, Friedlander M. Ovarian, fallopian tube, and peritoneal cancer. In: Berek JS, editor. Berek & Novak's gynecology. Philadelphia: Lippincott Williams & Wilkins; 2012. p. 682-748.
3. Mutch DG, DiSaia PJ. Germ cell, stromal, and other ovarian tumors. In: DiSaia PJ, Creasman WT, editors. Clinical gynecologic oncology. St. Louis: Mosby; 2012. p. 329-56.
4. Young RH. Sex cord-stromal, steroid cell, and other ovarian tumors with endocrine, paraendocrine, and paraneoplastic manifestations. In: Kurman RJ, Elleson LH, Ronnett BM, editors. Blaustein's pathology of the female genital tract. New York: Springer; 2010. p. 785-846.
5. Scully RE, Young RH, Clement PB. Sex cord-stromal tumors, granulosa cell tumors. In: Rosai J, Sobin LH, editors. Tumors of the ovary, maldeveloped gonads, fallopian tube, and broad ligament: atlas of tumor pathology. Washington, DC: Armed Forces Institute of Pathology; 1999. p. 169-88.
6. Kim SH, Kim SH. Granulosa cell tumor of the ovary: common findings and unusual appearances on CT and MR. J Comput Assist Tomogr 2002; 26: 756-61.
7. Rabban JT, Gupta D, Zaloudek CJ, Chen LM. Synchronous ovarian granulosa cell tumor and uterine serous carcinoma: a rare association of a high-risk endometrial cancer with an estrogenic ovarian tumor. Gynecol Oncol 2006; 103: 1164-8.
8. Sun HD, Lin H, Jao MS, Wang KL, Liou WS, Hung YC, et al. A long-term follow-up study of 176 cases with adult-type ovarian granulosa cell tumors. Gynecol Oncol 2012; 124: 244-9.
9. Morikawa K, Hatabu H, Togashi K, Kataoka ML, Mori T, Konishi J. Granulosa cell tumor of the ovary: MR findings. J Comput Assist Tomogr 1997; 21: 1001-4.
10. Dowdy SC, Mariani A, Lurain JR. Uterine cancer. In: Berek JS, editor. Berek & Novak's gynecology. Philadelphia: Lippincott Williams & Wilkins; 2012. p. 1250-303.
11. Takeuchi M, Matsuzaki K, Nishitani H. Diffusion-weighted magnetic resonance imaging of ovarian tumors: differentiation of benign and malignant solid components of ovarian masses. J Comput Assist Tomogr 2010; 34: 173-6.
12. Outwater EK, Wagner BJ, Mannion C, McLarney JK, Kim B. Sex cord-stromal and steroid cell tumors of the ovary. Radiographics 1998; 18: 1523-46.

-
- 
13. Kim JA, Chun YK, Moon MH, Lee YH, Cho HC, Lee MS, et al. High-resolution sonographic findings of ovarian granulosa cell tumors: correlation with pathologic findings. *J Ultrasound Med* 2010; **29**: 187-93.
 14. Nishino M, Hayakawa K, Iwasaku K, Togashi K, Ueda H, Sago T, et al. MR imaging of ovarian hemorrhage. *Eur J Radiol* 2004; **51**: 34-40.
 15. Koyama T, Togashi K. Functional MR imaging of the female pelvis. *J Magn Reson Imaging* 2007; **25**: 1101-12.
 16. Thomassin-Naggara I, Daraï E, Nassar-Slaba J, Cortez A, Marsault C, Bazot M. Value of dynamic enhanced magnetic resonance imaging for distinguishing between ovarian fibroma and subserous uterine leiomyoma. *J Comput Assist Tomogr* 2007; **31**: 236-42.
 17. Matsubayashi R, Matsuo Y, Doi J, Kudo S, Matsuguchi K, Sugimori H. Sclerosing stromal tumor of the ovary: radiologic findings. *Eur Radiol* 1999; **9**: 1335-8.
 18. Agha-Hosseini M, Aleyaseen A, Safdarian L, Kashani L. Secondary amenorrhea with low serum luteinizing hormone and follicle-stimulating hormone caused by an inhibin A- and inhibin B-producing granulosa cell tumor. *Taiwan J Obstet Gynecol* 2009; **48**: 72-5.
 19. Kuzbari O, Dorais J, Peterson CM. Endocrine Disorders. In: Berek JS, editor. *Berek & Novak's Gynecology*. Philadelphia: Lippincott Williams & Wilkins; 2012. p. 1066-132.
 20. Tanaka YO, Tsunoda H, Kitagawa Y, Ueno T, Yoshikawa H, Saida Y. Functioning ovarian tumors: direct and indirect findings at MR imaging. *Radiographics* 2004; **24(1)**: S147-66.